Hydrol. Earth Syst. Sci. Discuss., doi:10.5194/hess-2015-520, 2016
Manuscript under review for journal Hydrol. Earth Syst. Sci.
Published: 27 January 2016


Hydrology and Earth System Sciences
Open Access
Discussions

# Trends in evaporative demand in Great Britain using high-resolution meteorological data

**Emma L. Robinson[1], Eleanor M. Blyth[1], Douglas B. Clark[1], Jon Finch[1] and Alison C. Rudd[1]**

[1]{Centre for Ecology and Hydrology, Maclean Building, Benson Lane, Crowmarsh Gifford, Wallingford OX10 8BB}

Correspondence to: Emma L. Robinson (emrobi@ceh.ac.uk)

Hydrol. Earth Syst. Sci. Discuss., doi:10.5194/hess-2015-520, 2016
Manuscript under review for journal Hydrol. Earth Syst. Sci.
Published: 27 January 2016


**Abstract**

Observations of climate are often available on very different spatial scales from observations of the natural environments and resources that are affected by climate change. In order to help bridge the gap between these scales using modelling, a new dataset of daily meteorological variables was created at 1 km resolution over Great Britain for the years 1961-2012, by interpolating coarser resolution climate data and including the effect of local topography. These variables were used to calculate evaporative demand at the same spatial and temporal resolution, both excluding (PET) and including (PETI) the effect of water intercepted by the canopy. Temporal trends in evaporative demand were calculated, with PET found to increase in all regions and PETI found to increase in England. The trends were found to vary by season, with spring evaporative demand increasing by 14% (11% when the interception correction is included) in Great Britain over the dataset, while there is no statistically significant trend in other seasons. The trends in PET were attributed analytically to trends in the climate variables, with the spring trend in evaporative demand being driven by radiation trends, particularly by increasing solar radiation.

## 1 Introduction

There are many studies showing the ways in which our living environment is changing over time: wildlife surveys in the UK of both flora (Wood et al., 2015; Evans et al., 2008) and fauna (Pocock et al., 2015) show a shift in patterns and timing (Thackeray et al., 2010). In addition, the UK natural resources of freshwater (Watts et al., 2015), soils (Reynolds et al., 2013; Bellamy et al., 2005) and vegetation (Berry et al., 2002; Hickling et al., 2006; Norton et al., 2012) are changing. We are experiencing new environmental stresses on the land and water systems of the UK through changes in temperature and rainfall (Crooks and Kay, 2015; Watts et al., 2015; Hannaford, 2015).

To explain these changes in terms of physical drivers, there are several gridded meteorological datasets available for Great Britain. Some are derived directly from observations – for example the Met Office Rainfall and Evaporation Calculation System (MORECS) dataset (Thompson et al., 1981; Hough and Jones, 1997), the UKCP09 observed climate data (Jenkins et al., 2008) and the Climate Research Unit time series 3.21 (CRU TS 3.21) data (Jones and Harris, 2013; Harris et al., 2014) – while some use global meteorological reanalyses bias-corrected to observations – for example the WATCH Forcing Data (WFD; Weedon et al. (2011)),the WATCH Forcing Data methodology applied to ERA-Interim reanalysis product (WFDEI; Weedon et al. (2014)) and the Princeton Global Meteorological Forcing Dataset (Sheffield et al., 2006).

However, while observations of carbon, methane and water emissions from the land (Baldocchi et al., 1996), the vegetation cover (Morton et al., 2011) and soil properties (FAO/IIASA/ISRIC/ISS-CAS/JRC, 2012) are typically made at the finer landscape scale of 100 m to 1000 m, most long-term meteorological datasets are only available at a relatively coarse resolution of a few tens of km. These spatial scales may not be representative of the climate experienced by the flora and fauna being studied, and it has also been shown that input resolution can have a strong effect on the performance of hydrological models (Kay et al., 2015). In addition, the coarse temporal resolution of some datasets, for example the monthly CRU TS 3.21 data (Harris et al., 2014; Jones and Harris, 2013), can miss important sub-monthly extremes. It is imperative for our increased understanding and improved analysis of the environment that we bridge the gap between the scales of observations with modelling. However, while there are datasets available at higher spatial and temporal resolutions (such as

Hydrol. Earth Syst. Sci. Discuss., doi:10.5194/hess-2015-520, 2016
Manuscript under review for journal Hydrol. Earth Syst. Sci.
Published: 27 January 2016


Hydrology and Earth System Sciences Discussions

UKCP09 (Jenkins et al., 2008)), these often do not provide all the variables needed for land surface or hydrological modelling.

To address this, we have created a meteorological dataset for Great Britain at 1 km resolution (Robinson et al., 2015b). It is derived from the observation-based MORECS dataset (Thompson et al., 1981; Hough and Jones, 1997), which is downscaled using information about topography. This is augmented by an independent precipitation dataset – Gridded Estimates of daily and monthly Areal Rainfall for the United Kingdom (CEH-GEAR; Tanguy et al. (2014); Keller et al. (2015)) – along with variables from two global datasets – WFD Weedon et al. (2011) and CRU TS 3.21 (Harris et al., 2014; Jones and Harris, 2013) – to produce a comprehensive, observation-based, daily meteorological dataset at 1 km × 1 km spatial resolution.

In addition, a key variable in hydrological modelling is the evaporative demand of the atmosphere, which is determined by the meteorological variables (Kay et al., 2013). Hydrological models such as Climate and Land use Scenario Simulation in Catchments (CLASSIC; Crooks and Naden (2007)) or Grid-to-Grid (G2G; Bell et al. (2009)), and metrics such as the Palmer Drought Severity Index (PDSI; Palmer (1965)) require potential evapotranspiration (PET) – an estimate of the unstressed evaporative demand of the atmosphere – as an input. While hydrological models can make use of high resolution topographic information and precipitation datasets, they are often driven with PET calculated at a coarser resolution (Bell et al., 2011; Bell et al., 2012; Kay et al., 2015). Therefore, we have also created a dataset consisting of two estimates of PET, which can be used to run high-resolution hydrological models (Robinson et al., 2015a).

This paper presents the method of creation of the new high-resolution meteorological and PET datasets. Regional trends in evaporative demand are then calculated and attributed to regional trends in the meteorological data.

## 2 Calculation of meteorological variables

The meteorological variables included in this new dataset (Robinson et al., 2015b) are air temperature, specific humidity, wind speed, downward long- and shortwave radiation, precipitation, daily temperature range and air pressure (Table 1). These variables are important drivers of near-surface conditions, and are the full set of variables required to drive the JULES land surface model (LSM) (Best et al., 2011; Clark et al., 2011).

The data were derived primarily from MORECS, which is a long-term gridded dataset starting in 1961 and updated to the present (Thompson et al., 1981; Hough and Jones, 1997). It interpolates five daily synoptic station variables (air temperature, vapour pressure, wind speed, hours of bright sunshine, rainfall) to a 40 km × 40 km resolution grid aligned with the Ordnance Survey National Grid. The interpolation is such that the value in each grid square is the effective measurement of a station positioned at the centre of the square and at the grid square mean elevation, averaged from 09:00 GMT to 09:00 GMT the next day. MORECS is a consistent, quality-controlled time series, which accounts for changing station coverage. The MORECS variables were used to derive the air temperature, specific humidity, wind speed, downward long- and shortwave radiation and air pressure in the new dataset. The WFD and CRU TS 3.21 datasets were used where variables could not be calculated solely from MORECS, except for precipitation, for which the CEH-GEAR data were used instead of interpolating the MORECS rainfall.

The spatial coverage of the dataset was determined by the spatial coverage of MORECS, which covers the majority of Great Britain, but excludes some coastal regions and islands at the 1 km scale. For many of these points, the interpolation was extended from the nearest MORECS squares, but some outlying islands (in particular Shetland and the Scilly Isles) were deemed to be too far from any MORECS squares and were therefore excluded.

### 2.1 Air temperature

Air temperature, $T_a$ (K), was derived from the MORECS air temperature. The MORECS air temperature was reduced to mean sea level, using a lapse rate of -0.006 K m$^{-1}$ (Hough and Jones, 1997). A bicubic spline was used to interpolate from 40 km resolution to 1 km resolution, then the temperatures were adjusted to the elevation of each 1 km square using the same lapse rate. The 1 km resolution elevation data were aggregated from the Integrated Hydrological Digital Terrain Model (IHDTM) – a 50 m resolution digital terrain model (Morris and Flavin, 1990).

### 2.2 Specific humidity

Specific humidity, $q_a$ (kg kg$^{-1}$), was derived from the MORECS vapour pressure, which was first reduced to mean sea level, using a lapse rate of -0.025 % m$^{-1}$ (Hough and Jones, 1997). A bicubic spline was used to interpolate to 1 km resolution then the vapour pressure values were adjusted to the 1 km resolution elevation using the IHDTM elevations (Sect. 2.1). Finally the specific humidity was calculated, assuming a constant air pressure, $p_* = 100000$ Pa, using

$$q_a = \frac{\epsilon e}{p_* - (1-\epsilon)e}, \quad (1)$$

where $e$ is the vapour pressure (Pa) and $\epsilon = 0.622$ is the mass ratio of water to dry air (Gill, 1982).

## 2.3 Downward shortwave radiation

Downward shortwave radiation, $S_d$ (W m$^{-2}$), was derived from the MORECS hours of bright sunshine. The value calculated is the mean shortwave radiation over 24 hours. The sunshine hours were used to calculate the cloud cover factor, $C_f = n/N$, where $n$ is the number of hours of bright sunshine in a day, and $N$ is the total number of hours between sunrise and sunset. The cloud cover factor was interpolated to 1 km resolution using a bicubic spline. The downward shortwave solar radiation for a horizontal plane at the Earth's surface was calculated using the solar angle equations of Iqbal (1983) and a form of the Angstrom-Prescott equation which relates hours of bright sunshine to solar irradiance (Ångström, 1918; Prescott, 1940), with empirical coefficients calculated by Cowley (1978). The Cowley coefficients vary spatially and seasonally and effectively account for reduction of irradiance with increasing solar zenith angle, as well as implicitly accounting for spatially- and seasonally-varying aerosol effects. However, they do not vary interannually and thus do not explicitly include long-term trends in aerosol concentration.

In addition, the downward shortwave radiation was corrected for the average inclination and aspect of the surface, assuming that only the direct beam radiation is a function of the inclination and that the diffuse radiation is homogeneous. It was also assumed that the cloud cover is the dominant factor in determining the diffuse fraction (Muneer and Munawwar, 2006). The aspect and inclination were calculated using the IHDTM elevation at 50 m resolution, following the method of Horn (1981), and were then aggregated to 1 km resolution. The top of atmosphere flux for horizontal and inclined surfaces was calculated following Allen et al. (2006) and the ratio used to scale the direct beam radiation.

### 2.4 Downward longwave radiation

Downward longwave radiation, $L_d$ (W m$^{-2}$), was derived from the 1 km resolution air temperature (Sect. 2.1), vapour pressure (Sect. 2.2) and cloud cover factor (Sect. 2.3). The downward longwave radiation for clear sky conditions was calculated as a function of air temperature and precipitable water using the method of Dilley and O'Brien (1998), with precipitable water calculated from air temperature and humidity following Prata (1996). The additional component due to cloud cover was calculated using the equations of Kimball et al. (1982), assuming a constant cloud base height of 1000 m.

### 2.5 Wind speed

The 10 m wind speed, $u_{10}$ (m s$^{-1}$), was derived from the MORECS 10 m wind speed. The MORECS wind speed data were interpolated to 1 km resolution using a bicubic spline and adjusted for topography using a 1 km resolution dataset of mean wind speeds produced by the UK Energy Technology Support Unit (ETSU) (Newton and Burch, 1985; Burch and Ravenscroft, 1992). This used Numerical Objective Analysis Boundary Layer (NOABL) methodology and station wind measurements over the period 1975-84 to produce a map of mean wind speed over the UK. To calculate the topographic correction, the ETSU wind speed was aggregated to 40 km resolution, then the difference between each 1 km value and the corresponding 40 km mean found. This difference was added to the interpolated daily wind speed.

### 2.6 Precipitation

Precipitation, $P$ (kg m$^{-2}$ s$^{-1}$), is taken from the daily CEH-GEAR dataset (Tanguy et al., 2014; Keller et al., 2015), scaled to the appropriate units. The CEH-GEAR methodology uses natural neighbour interpolation to interpolate synoptic station data to a 1 km resolution gridded daily precipitation dataset of the estimated rainfall in 24 hours between 09:00 GMT and 09:00 GMT the next day.

### 2.7 Daily temperature range

Daily temperature range (DTR), $D_T$ (K), was obtained from the CRU TS 3.21 monthly mean daily temperature range estimates on a 0.5° latitude × 0.5° longitude grid, which is interpolated from monthly climate observations (Harris et al., 2014; Jones and Harris, 2013). These data were reprojected to the 1 km grid with no interpolation and the monthly mean used to populate the daily values in each month.

### 2.8 Surface air pressure

Surface air pressure, $p_*$ (Pa), was derived from the WFD, an observation-corrected reanalysis product, which provides 3 hourly meteorological data for 1958-2001 on a 0.5° latitude × 0.5° longitude resolution grid (Weedon et al., 2011). Mean monthly values of WFD surface air pressure and air temperature were calculated for each 0.5° grid box over the years 1961-2001. These were reprojected to the 1 km grid with no interpolation, then the air temperature used to lapse the air pressure from the WFD elevation to the 1 km resolution elevation using the temperature lapse rate specified in Sect. 2.1 (Shuttleworth, 2012). The mean monthly values were used to populate the daily values in the full dataset, thus the surface air pressure in the new dataset does not vary interanually. This is reasonable as the trend in surface air pressure in the WFD is negligible.

### 2.9 Spatial and seasonal patterns of meteorological variables

Long-term mean values of each meteorological variable were calculated for each 1 km square over the whole dataset (1961-2012) (Fig. 1). Mean-monthly climatologies (Fig. 2) were calculated over the whole of Great Britain (GB), and over four sub-regions of interest (Fig. 3). Three of these regions correspond to the nations (England, Wales and Scotland), while the fourth is the ‘English lowlands’, a subset of the English region, which includes south-central and south-east England, East Anglia and the East Midlands (Folland et al., 2015).

The maps clearly show the effect of topography on the variables (Fig. 1), with an inverse correlation between elevation and temperature, specific humidity, downward longwave radiation and surface air pressure and a positive correlation with wind speed. The precipitation has an east-west gradient due to prevailing weather systems and orography. The fine-scale structure of the downward shortwave radiation is due to the aspect and elevation of each grid cell, with more spatial variability in areas with more varying terrain. As no topographic correction has been applied to DTR, it varies only on a larger spatial scale.

The mean-monthly climatologies (Fig. 2) demonstrate the differences between the regions, with Scotland generally having lower temperatures and more precipitation than the average, and England (particularly the English lowlands) being warmer and drier.

## 3 Calculation of potential evapotranspiration (PET)

The Penman-Monteith PET, $E_P$ (mm d$^{-1}$, equivalent to kg m$^{-2}$ d$^{-1}$), is a physically-based formulation of the evaporative demand of the atmosphere (Monteith, 1965). It is calculated from the daily meteorological variables using the equation

$$E_P = \frac{t_d}{\lambda}\frac{\Delta A+\frac{c_p\rho_a}{r_a}(q_s-q_a)}{\Delta+\gamma\left(1-\frac{r_s}{r_a}\right)}, \quad (2)$$

where $t_d$ = 86400 s d$^{-1}$ is the length of a day, $\lambda$=2.5×10$^6$ J kg$^{-1}$ is the latent heat of evaporation, $q_s$ is saturated specific humidity (kg kg$^{-1}$), Δ is the gradient of saturated specific humidity with respect to temperature (kg kg$^{-1}$ K$^{-1}$), $A$ is the available energy (W m$^{-2}$), $c_p$=1010 J kg$^{-1}$ K$^{-1}$ is the specific heat capacity of air, $\rho_a$ is the density of air (kg m$^{-3}$), $q$ is specific humidity (kg kg$^{-1}$), $\gamma$=0.004 K$^{-1}$ is the psychrometric constant, $r_s$ is stomatal resistance (s m$^{-1}$) and $r_a$ is aerodynamic resistance (s m$^{-1}$) (Stewart, 1989).

The saturated specific humidity, $q_s$ (kg kg$^{-1}$), is calculated from saturated vapour pressure, $e_s$ (Pa), using Eq. (1). The saturated vapour pressure is calculated using an empirical fit to air temperature

$$e_s = p_s exp\left(\sum_{i=1}^{4} a_i\left(1-\frac{T_s}{T_a}\right)^i\right), \quad (3)$$

where $p_s$ = 101325 Pa is the steam point pressure, $T_s$ = 373.15 K is the steam point temperature and $a$=(13.3185, -1.9760, -0.6445, -0.1299) are empirical coefficients (Richards, 1971).

The derivative of the saturated specific humidity with respect to temperature, Δ (kg kg$^{-1}$ K$^{-1}$), is therefore

$$\Delta = \frac{T_s}{T_a^2}\frac{p_* q_s}{p_*-(1-\epsilon)e_s}\sum_{i=1}^{4} i a_i\left(1-\frac{T_s}{T_a}\right)^i. \quad (4)$$

The available energy, $A$ (W m$^{-2}$), is the energy balance of the surface,

$$A = R_n - G, \quad (5)$$

where $R_n$ is the net radiation (W m$^{-2}$) and $G$ is the soil heat flux (W m$^{-2}$). The net soil heat flux is negligible at the daily timescale (Allen et al., 1998), so the available energy is equal to the net radiation, such that

$$A = (1-\alpha)S_d + \varepsilon(L_d - \sigma T_*^4), \quad (6)$$

where $\sigma$ is the Stefan-Boltzmann constant, $\alpha$ is the albedo and $\varepsilon$ the emissivity of the surface and $T_*$ is the surface temperature (Shuttleworth, 2012). For this study the surface temperature is approximated by using the air temperature, $T_a$. The albedo and emissivity are also dependent on the land cover; for a well-watered grass surface an albedo of 0.23 and an emissivity of 0.92 are used (Allen et al., 1998).

The air density, $\rho_a$ (kg m$^{-3}$), is a function of air pressure and temperature,

$$\rho_a = \frac{p_*}{rT_a}, \quad (7)$$

where $r$ = 287.05 J kg$^{-1}$ K$^{-1}$ is the gas constant of air.

The stomatal and aerodynamic resistances are strongly dependent on the land cover due to differences in roughness length and physiological constraints on transpiration of different vegetation types. As a standard, the Food and Agriculture Organization of the United Nations (FAO) recommend the use of PET calculated for a hypothetical reference crop, which corresponds to a well-watered grass crop of 0.12 m height, with constant stomatal resistance, $r_s$ = 70.0 s m$^{-1}$ (Allen et al., 1998). Following this recommendation, the PET in the current study was calculated for the reference crop over the whole of Great Britain. If necessary, this can be adjusted to give an estimate of PET specific to the local land cover, for example using regression relationships (Crooks and Naden, 2007).

Following Allen et al. (1998), aerodynamic resistance, $r_a$ (s m$^{-1}$), is a function of the 10 m wind speed

$$r_a = \frac{278}{u_{10}}. \quad (8)$$

Thus the PET is a function of six of the meteorological variables: air temperature, specific humidity, downward long- and shortwave radiation and surface air pressure.

The PET can be split between two factors, the radiative component, $E_{PR}$,

$$E_{PR} = \frac{t_d}{\lambda} \frac{\Delta A}{\Delta + \gamma\left(1 - \frac{r_s}{r_a}\right)}, \quad (9)$$

and the aerodynamic component, $E_{PA}$,

$$E_{PA} = \frac{t_d}{\lambda} \frac{\frac{c_p \rho_a}{r_a}(q_s - q_a)}{\Delta + \gamma\left(1 - \frac{r_s}{r_a}\right)}, \quad (10)$$

such that $E_P$=$E_{PR}$+$E_{PA}$.

Hydrol. Earth Syst. Sci. Discuss., doi:10.5194/hess-2015-520, 2016
Manuscript under review for journal Hydrol. Earth Syst. Sci.
Published: 27 January 2016

Hydrology and Earth System Sciences
Discussions

### 3.1 Potential evapotranspiration plus interception (PETI)

When rain falls, water is intercepted by the canopy. The evaporation of this intercepted water is subject to the same aerodynamic resistance, defined by the roughness of the canopy, as transpiration, but is not constrained by stomatal resistance (Shuttleworth, 2012). At the same time, leaves covered with water cannot transpire, so interception inhibits transpiration from the wet fraction of the canopy (Ward and Robinson, 2000). In the short term after a rain event, potential water losses due to evaporation may be underestimated if only potential transpiration is calculated. This can be accounted for by introducing an interception term to the calculation of PET. If the daily rainfall is greater than zero, then the rain is used to fill (part of) the canopy and this store evaporates as interception, inhibiting the transpiration. On days without rain, the potential is equal to the PET defined in Eq. 2. A similar correction is applied to the PET provided at 40 km resolution by MORECS (Thompson et al., 1981).

The potential evapotranspiration plus interception (PETI) is a function of the PET, $E_P$, (as calculated above) and potential interception, $E_I$, which is calculated by substituting $r_s$=0 s m$^{-1}$ into Eq. (2). To calculate the relative proportions of interception and transpiration, it is assumed that the wet fraction of the canopy is proportional to the amount of water in the interception store and that transpiration is only possible through the fraction of the canopy which is dry. The interception store, $S_I$ (kg m$^{-2}$), decreases through the day according to an exponential dry down (Rutter et al., 1971), such that

$$S_I(t) = S_o e^{-\frac{E_I}{S_{tot}}t}, \tag{11}$$

where $E_I$ is the potential interception, $S_{tot}$ is the total capacity of the interception store (kg m$^{-2}$), $S_0$ is the precipitation that is intercepted by the canopy (kg m$^{-2}$) and $t$ is the time (in days) since a rain event. The total capacity of the interception store is calculated following Best et al. (2011), such that

$$S_{tot} = 0.5 + 0.05\Lambda, \tag{12}$$

where $\Lambda$ is the leaf area index (LAI); for the FAO standard grass land cover the LAI is 2.88 (Allen et al., 1998). The fraction of rainfall intercepted by the canopy is found also following Best et al. (2011), assuming that rainfall lasts for an average of 3 hours.

The wet fraction of the canopy, $C_{wet}$, is proportional to the store size, such that

$$C_{wet}(t) = \frac{S(t)}{S_{tot}}. \tag{13}$$

Hydrol. Earth Syst. Sci. Discuss., doi:10.5194/hess-2015-520, 2016
Manuscript under review for journal Hydrol. Earth Syst. Sci.
Published: 27 January 2016

Hydrology and Earth System Sciences Discussions

The total PETI is the sum of the interception from the wet canopy and the transpiration from the dry canopy,

$$E_{PI}(t) = E_I C_{wet}(t) + E_P\big(1 - C_{wet}(t)\big). \quad (14)$$

This is integrated over one day to find the total PETI, $E_{PI}$ (mm d$^{-1}$), to be

$$E_{PI} = S_0\left(1 - e^{-\frac{E_I}{S_{tot}}}\right) + E_P\left(1 - \frac{S_0}{E_I}\left(1 - e^{-\frac{E_I}{S_{tot}}}\right)\right). \quad (15)$$

The PETI is a function of the same six meteorological variables as the PET, plus the precipitation.

## 3.2 Spatial and seasonal patterns of potential evapotranspiration

Both PET and PETI have a distinct gradient from low in the north-west to high in the south-east, and they are both inversely proportional to the elevation (Fig. 4), reflecting the spatial patterns of the meteorological variables. The PETI is higher than the PET overall but this difference is larger in the north and west, where precipitation rates, and therefore interception, are higher (Fig. 4). In Scotland, the higher interception and lower evaporative demand mean that this increase is a larger proportion of the total, with the mean PETI being 10% larger than the PET (in some areas the difference is more than 25%). In the English lowlands the difference is more moderate, at 6%, but it is a more water limited region where hydrological modelling can be sensitive to even relatively small adjustments to PET (Kay et al., 2013).

The seasonal climatology of both PET and PETI follow the meteorology (Fig. 5), with high values in the summer and low in the winter. The absolute difference between PET and PETI is bimodal, with a peak in March and a smaller peak in October (September in Scotland) (Fig. 5), because in winter the overall evaporative demand is low, while in summer the amount of rainfall is low, so the interception correction is small. The seasonal cycle of PET is driven predominantly by the radiative component, which has a much stronger seasonality than the aerodynamic component (Fig. 6).

On a monthly or annual timescale, the ratio of PET to precipitation is an indicator of the wet- or dryness of a region (Kay et al., 2013). Low values of PET relative to precipitation indicate wet regions, where evaporation is demand-limited, while high values indicate dry, water-limited regions. In the wetter regions (Scotland, Wales) mean-monthly PET and PETI (Fig. 5) are on average lower than the mean-monthly precipitation (Fig. 2) throughout the year, while

Hydrol. Earth Syst. Sci. Discuss., doi:10.5194/hess-2015-520, 2016
Manuscript under review for journal Hydrol. Earth Syst. Sci.
Published: 27 January 2016

Hydrology and Earth System Sciences
Open Access
Discussions

in drier regions (England, English lowlands) the PET and PETI are higher than the precipitation for much of the summer, highlighting the region's susceptibility to hydrological drought (Folland et al., 2015).

## 4 Decadal trends

Annual means of the meteorological variables (Fig. 7) and the PET and PETI (Fig. 8) were calculated for each of the five regions. The trends in these annual means were calculated using linear regression; the significance (*P* value) and 95% confidence intervals of the slope are calculated assuming a non-zero lag-1 autocorrelation, to account for possible correlation between adjacent data points (von Storch and Zwiers, 1999; Zwiers and von Storch, 1995). In addition, seasonal means were calculated, with the four seasons defined to be December-February, March-May, June-August and September-November, and trends in these means were also found.

The trends and associated 95% confidence intervals of the annual means for Great Britain of the meteorological variables can be seen in Table 2. The trends in the annual and seasonal means for all regions are plotted in Fig. 9; trends that are statistically significant at the 5% level are plotted with solid error bars, those that are not significant are plotted with dashed lines. There was a statistically significant trend in air temperature in all regions (except in winter), which agrees with recent trends in the Hadley Centre Central England Temperature (HadCET) dataset (Parker and Horton, 2005) and in temperature records for Scotland (Jenkins et al., 2008) as well as in the CRUTEM4 dataset (Jones et al., 2012). An increase in winter precipitation in Scotland is seen in the current dataset, but no significant trends otherwise. Long term observations show that there has been little trend in annual precipitation, but a change in seasonality with wetting winters and drying summers (Jenkins et al., 2008). The statistically significant decline in wind speed in all regions is consistent with the results of McVicar et al. (2012) and Vautard et al. (2010), who report decreasing wind speeds in the northern hemisphere over the late 20$^{th}$ century.

The slopes and associated 95 % confidence intervals of PET and PETI for annual means over Great Britain can be seen in Table 2, and the trends in the annual and seasonal means of PET, PETI, and the radiative and aerodynamic components of PET are plotted in Fig. 10 for all regions. There is a statistically significant increase in annual PET in all regions except Wales; the GB trend (0.021 mm d$^{-1}$ decade$^{-1}$) is equivalent to an increase of 0.11 mm d$^{-1}$ (8 % of the long term mean) over the whole dataset. Increases in PETI are only statistically significant in

Hydrol. Earth Syst. Sci. Discuss., doi:10.5194/hess-2015-520, 2016
Manuscript under review for journal Hydrol. Earth Syst. Sci.
Published: 27 January 2016


England (0.023 mm $d^{-1}$ $decade^{-1}$) and English lowlands (0.028 mm $d^{-1}$ $decade^{-1}$), where the increases over the whole dataset are 0.12 mm $d^{-1}$ (8% of the long term mean) and 0.15 mm $d^{-1}$ (10 % of the long term mean) respectively. There is a difference in trend between different seasons. In winter, summer and autumn there are no statistically significant trends in PET or PETI, other than the English lowlands in autumn, but the spring is markedly different, with very significant trends ($P$<0.0005) in all regions. The GB spring trends in PET (0.043 mm $d^{-1}$ $decade^{-1}$) and PETI (0.038 mm $d^{-1}$ $decade^{-1}$) are equivalent to an increase of 0.22 mm $d^{-1}$ (14 % of the long-term spring mean) and 0.20 mm $d^{-1}$ (11 % of the long-term spring mean) over the length of the dataset respectively. The radiative component of PET has similarly significant trends in spring, while the aerodynamic component has no significant trends in any season (Fig. 10), indicating that the trend in PET is due to the increasing radiative component.

There are few studies of long-term trends in evaporative demand in the UK. MORECS provides an estimate of Penman-Monteith PET calculated directly from the 40 km resolution meteorological data (Hough and Jones, 1997; Thompson et al., 1981), and increases can be seen over the dataset (Rodda and Marsh, 2011). But as the PET and PETI in the current dataset are ultimately calculated using the same meteorological data (albeit by different methods), it is not unexpected that similar trends should be seen. Site-based studies suggest an increase over recent decades (Burt and Shahgedanova, 1998; Crane and Hudson, 1997), but it is difficult to separate climate-driven trends from local land-use trends. The global review paper by (McVicar et al., 2012) identifies a trend of decreasing evaporative demand in the northern hemisphere, driven by decreasing wind speeds, however they also report significant local variations on trends in pan evaporation, including the increasing trend observed by Stanhill and Möller (2008) at a site in England after 1968. Matsoukas et al. (2011) identify a statistically significant increase in P in several regions of the globe, including southern England, between 1983 and 2008, attributing it predominantly to an increase in the radiative component of PET, due to global brightening.

Regional changes in actual evaporative losses can be estimated indirectly using regional precipitation and runoff or river flow. Using a combination of observations and modelling, Marsh and Dixon (2012) identified an increase in evaporative losses in Great Britain from 1961-2011. Hannaford and Buys (2012) note seasonal and regional differences in trends in observed river flow, suggesting that decreasing spring flows in the English lowlands are indicative of increasing evaporative demand. However, changing evaporative losses can also be due to changing supply through precipitation, so it is important to formally attribute the trends in PET to changing climate, in order to understand changing evaporative losses.

### 4.1 Attribution of trends in potential evapotranspiration

In order to attribute changes in PET to changes in climate, the rate of change of PET, d$E_p$/d$t$, can be calculated as a function of the rate of change of each variable (Donohue et al., 2010),

$$\frac{\mathrm{d}E_P}{\mathrm{d}t} = \frac{\mathrm{d}E_P}{\mathrm{d}T_a}\frac{\mathrm{d}T_a}{\mathrm{d}t} + \frac{\mathrm{d}E_P}{\mathrm{d}q_a}\frac{\mathrm{d}q_a}{\mathrm{d}t} + \frac{\mathrm{d}E_P}{\mathrm{d}u_{10}}\frac{\mathrm{d}u_{10}}{\mathrm{d}t} + \frac{\mathrm{d}E_P}{\mathrm{d}L_d}\frac{\mathrm{d}L_d}{\mathrm{d}t} + \frac{\mathrm{d}E_P}{\mathrm{d}S_d}\frac{\mathrm{d}S_d}{\mathrm{d}t}. \tag{16}$$

Note that we exclude the surface air pressure, as the interannual variability of air pressure is negligible. The derivative of the PET with respect to each of the meteorological variables can be found analytically (Appendix A). The derivatives are calculated from the daily meteorological data, then the overall annual and regional means found. Substituting the slopes of the linear regressions of the annual means (Fig. 9) for the rate of change of each variable with time, the contribution of each variable to the rate of change of PET can be calculated. The same can also be applied to the radiative and aerodynamic components independently.

Figure 11 shows the contribution of each meteorological variable to the rate of change of the annual mean PET and to the radiative and aerodynamic components. The percentage contribution is seen in Table 3. The radiative component has no dependence on specific humidity, while the aerodynamic component has no dependence on long- or shortwave radiation.

The rate of change of PET is almost entirely due to the change in the radiative component. In all regions except Scotland, the change in the radiative component of PET is dominated by the increase due to the increasing downward shortwave radiation, followed by the increasing downward longwave radiation, while in Scotland the effect of the downward shortwave is smaller. In all regions there is also a small increase in the radiative component due to the decreasing wind speed, and a decrease due to increasing air temperature, but these are negligible compared to the effect of changing radiation. Increasing air temperature contributes to a small increase in the aerodynamic component of PET, but this is offset by the decrease due to increasing specific humidity and decreasing wind speed, so that overall the change in the aerodynamic component is negligible.

Hydrol. Earth Syst. Sci. Discuss., doi:10.5194/hess-2015-520, 2016
Manuscript under review for journal Hydrol. Earth Syst. Sci.
Published: 27 January 2016

Hydrology and Earth System Sciences
Open Access
Discussions

## 5 Discussion

These high resolution datasets provide an insight into the effect of the changing climate of Great Britain on evaporative demand over the past five decades. There have been significant climatic trends in the UK since 1961; in particular rising air temperature and specific humidity, decreasing wind speed and decreasing cloudiness. The resulting trends in downward long- and shortwave radiation have combined to lead to trends in evaporative demand.

Wind speeds have decreased more significantly in the west than the east, and show a consistent decrease across seasons. Contrary to Donohue et al. (2010) and McVicar et al. (2012), this study finds that the change in wind speed of the late 20$^{th}$ and early 21$^{st}$ centuries has had a negligible influence on PET over the period of study. However, the previous studies were concerned with open-water Penman evaporation, which has a simpler (proportional) dependence on wind speed than the Penman-Monteith PET considered here. Although the significant decrease in wind speed has had a negligible effect on evaporative demand, it may nonetheless have had a direct effect on biodiversity (Barton, 2014; Brittain et al., 2013) and implications for wind energy resources (Sinden, 2007).

The air temperature trends in this study of around 0.2 K decade$^{-1}$ are consistent with observed global and regional trends (Hartmann et al., 2013; Jenkins et al., 2008). The temperature trend also does not explicitly make a large contribution to the trend in PET, but is partly responsible for the trend of increasing downward longwave radiation. The trends in longwave radiation in these datasets are not statistically significant, due to high inter-annual variability, but contribute to between 22% and 50% of the trends in PET and the radiative component (Table 3). Observations of longwave radiation are often uncertain, but, although small, the trend in this dataset is consistent with observed trends (Wang and Liang, 2009), as well as with trends in the WFDEI bias-corrected reanalysis product (Weedon et al., 2014).

Increasing solar radiation has been shown to have a strong effect on spring and annual evaporative demand, contributing to between 46% and 77% of the trend in annual PET (Table 3), increasing to between 84% and 87% of the trend in spring PET. Two main mechanisms can be responsible for changing solar radiation – changing cloud cover and changing aerosol concentrations. Changing aerosol emissions have been shown to have had a significant effect on solar radiation in the 20$^{th}$ century. In Europe, global dimming due to increased aerosol concentrations peaked around 1980, followed by global brightening as aerosol concentrations decreased (Wild, 2009). Observations of changing continental runoff and river flow in Europe over the 20th century have been attributed to changing aerosol concentrations, via their effect on solar radiation, and thus evaporative demand (Gedney et al., 2014).

In this study we use the duration of bright sunshine to calculate the solar radiation, using empirical coefficients which do not vary with year, so aerosol effects are not explicitly included. The coefficients used in this study to convert sunshine hours to radiation fluxes were empirically derived in 1978; the derivation used data from the decade 1966-75, as this period was identified to be before reductions in aerosol emissions had begun to significantly increase observed solar radiation (Cowley, 1978). Despite this, the trend in shortwave radiation in the current dataset from 1979 onwards is consistent, within uncertainties, with that seen in the WFDEI data, which is bias-corrected to observations and includes explicit aerosol effects (Weedon et al., 2014).

It has been suggested that aerosol effects also implicitly affect sunshine duration (Helmes and Jaenicke, 1986). Several regional studies have shown trends in sunshine hours that are consistent with the periods of dimming and brightening across the globe (eg Liley, 2009; Sanchez-Lorenzo et al., 2009; Sanchez-Lorenzo et al., 2008; Stanhill and Cohen, 2005), and several have attempted to quantify the relative contribution of trends in cloud cover and aerosol loading (e.g. Sanchez-Lorenzo and Wild (2012) in Switzerland, see Sanchez-Romero et al. (2014) for a review). Therefore, it may be that some of the brightening trend seen in the current dataset is due to the implicit signal of aerosol trends in the MORECS sunshine duration, although this is likely to be small compared to the effects of changing cloud cover.

The trends in the MORECS sunshine duration used in this study are consistent with changing weather patterns which may be attributed to the Atlantic Multidecadal Oscillation (AMO). The AMO has been shown to cause a decrease in spring precipitation (and therefore cloud cover) in northern Europe over recent decades (Sutton and Dong, 2012), and the trend in MORECS sunshine hours is dominated by an increase in the spring mean. This has also been seen in Europe-wide sunshine hours data (Sanchez-Lorenzo et al., 2008). On the other hand, the effect of changing aerosols on sunshine hours is expected to be largest in the winter (Sanchez-Lorenzo et al., 2008). However, it would not be possible to directly identify either of these effects on the sunshine duration without access to longer data records.

The inclusion of explicit aerosol effects in the coefficients of the Angstrom-Prescott equation would be expected to mitigate the trend in evaporative demand in the first two decades of the dataset, and enhance it after 1980. Gedney et al. (2014) attribute a decrease in European solar

Hydrol. Earth Syst. Sci. Discuss., doi:10.5194/hess-2015-520, 2016
Manuscript under review for journal Hydrol. Earth Syst. Sci.
Published: 27 January 2016


Hydrology and Earth System Sciences
Discussions

radiation of 10 W $m^{-2}$ between the periods 1901-10 and 1974-80, and an increase of 4 W $m^{-2}$ from 1974-84 to1990-99 to changing aerosol contributions. Applying these trends to the current dataset, with a turning point at 1980, would double the overall increase in solar radiation in Great Britain, which would lead to a 50 % increase in the overall trend in PET.

The trends in temperature and cloud cover in the UK are expected to continue into the coming decades, with precipitation expected to increase in the winter but decrease in the summer (Murphy et al., 2009). Therefore it is likely that evaporative demand will increase, increasing water stress in the summer when precipitation is lower and potentially affecting water resources, agriculture and biodiversity. This has been demonstrated for southern England and Wales by Rudd and Kay (2015), who calculated present and future PET using high-resolution RCM output and include $CO_2$ fertilisation.

The current study is concerned only with the effects of changing climate on evaporative demand and has assumed a constant bulk canopy resistance throughout. However, plants are expected to react to increased $CO_2$ in the atmosphere by closing stomata and limiting the exchange of gases, including water (Kruijt et al., 2008), and observed changes in runoff have been attributed to this effect (Gedney et al., 2006; Gedney et al., 2014). It is possible that the resulting change of canopy resistance could partially offset the increased atmospheric demand (Rudd and Kay, 2015) and may impact runoff (Gedney et al., 2006; Prudhomme et al., 2014), but further studies would be required to quantify this.

This paper has presented a unique high-resolution observation-based dataset of meteorological variables and evaporative demand in Great Britain since 1961. We have shown that trends in evaporative demand can be attributed to trends in the meteorological variables. The meteorological variables provided are sufficient to run land surface models and combined with the PET can be used to run hydrological models. In addition, the high spatial (1km) and temporal (daily) resolution will allow this dataset to be used to study the effects of climate on physical and biological systems at a range of scales, from local to national.

## Author contribution

EB, JF and DBC designed the study. JF, ACR, DBC and ELR developed code to create meteorological data. ELR created the PET and PETI. ELR and EB analysed trends. ELR, EB, ACR and DBC wrote the manuscript.

## Acknowledgements

Hydrol. Earth Syst. Sci. Discuss., doi:10.5194/hess-2015-520, 2016
Manuscript under review for journal Hydrol. Earth Syst. Sci.
Published: 27 January 2016


Hydrology and Earth System Sciences
Discussions
Open Access

The meteorological variables presented are based largely on GB meteorological data under licence from the Met Office, and those organisations contributing to this national dataset (including the Met Office, Environment Agency, Scottish Environment Protection Agency (SEPA) and Natural Resources Wales) are gratefully acknowledged. The CRU TS 3.21 daily temperature range data were created by the University of East Anglia Climatic Research Unit, and the WFD air pressure data were created as part of the EU FP6 project WATCH (Contract 036946). Thanks to Nicola Gedney and Graham Weedon for useful discussions.

This work was funded by the Natural Environment Research Council in the Changing Water Cycle programme: NERC Reference: NE/I006087/1.

Hydrol. Earth Syst. Sci. Discuss., doi:10.5194/hess-2015-520, 2016
Manuscript under review for journal Hydrol. Earth Syst. Sci.
Published: 27 January 2016


Hydrology and Earth System Sciences
Discussions
Open Access

## Appendix A: Derivatives of potential evapotranspiration

The wind speed affects the PET through the aerodynamic resistance. The derivative with respect to wind speed is

$$\frac{\partial E_P}{\partial u_{10}} = \frac{(\Delta+\gamma)E_{PA} - \gamma\frac{r_s}{r_a}E_{PR}}{u_{10}\left(\Delta+\gamma\left(1+\frac{r_s}{r_a}\right)\right)} . \tag{A1}$$

The downward long- and shortwave radiation affect PET through the net radiation, and the derivatives are

$$\frac{\partial E_P}{\partial L_d} = E_{PR}\frac{\epsilon}{R_n} \tag{A2}$$

$$\frac{\partial E_P}{\partial S_d} = E_{PR}\frac{(1-\alpha)}{R_n} . \tag{A3}$$

The derivative of PET with respect to specific humidity is

$$\frac{\partial E_P}{\partial q_a} = \frac{E_{PA}}{q_a - q_s} . \tag{A4}$$

The air temperature affects PET through the saturated specific humidity and its derivative, the net radiation and the air density, so that the derivative of PET with respect to air temperature is

$$\frac{\partial E_P}{\partial T_a} = E_{PR}\left(\frac{\gamma\left(1+\frac{r_s}{r_a}\right)}{T_a^2\left(\Delta+\gamma\left(1+\frac{r_s}{r_a}\right)\right)}\left[T_{sp}\left(\sum_{i=1}^{4} i a_i T_r^{i-1} + \frac{\sum_{i=1}^{4} i a_i T_r^{i-1}}{\sum_{i=1}^{4} i(i-1) a_i T_r^{i-2}} + \frac{2(1-\varepsilon)\sum_{i=1}^{4} i a_i T_r^{i-1} q_s}{\varepsilon}\right) - 2T_a\right] - \frac{4\epsilon\sigma T_a^4}{R_n}\right) + E_{PA}\left(\frac{\Delta}{q_s - q} - \frac{1}{T_a} - \frac{\Delta}{T_a^2\left(\Delta+\gamma\left(1+\frac{r_s}{r_a}\right)\right)}\left[T_{sp}\left(\sum_{i=1}^{4} i a_i T_r^{i-1} + \frac{\sum_{i=1}^{4} i a_i T_r^{i-1}}{\sum_{i=1}^{4} i(i-1) a_i T_r^{i-2}} + \frac{2(1-\varepsilon)\sum_{i=1}^{4} i a_i T_r^{i-1} q_s}{\varepsilon}\right) - 2T_a\right]\right) . \tag{A5}$$

## 6 References

Allen, R. G., Pereira, L. S., Raes, D., and Smith, M.: Crop evapotranspiration - Guidelines for computing crop water requirements, Food and Agriculture Organization of the United Nations, Rome, Italy, FAO Irrigation and Drainage Paper, 1998.

Allen, R. G., Trezza, R., and Tasumi, M.: Analytical integrated functions for daily solar radiation on slopes, Agr Forest Meteorol, 139, 55-73, doi:10.1016/j.agrformet.2006.05.012, 2006.

Ångström, A.: A study of the radiation of the atmosphere, Smithsonian Miscellaneous Collections, 65, 159-161, 1918.

Baldocchi, D., Valentini, R., Running, S., Oechel, W., and Dahlman, R.: Strategies for measuring and modelling carbon dioxide and water vapour fluxes over terrestrial ecosystems, Global Change Biology, 2, 159-168, doi:10.1111/j.1365-2486.1996.tb00069.x, 1996.

Barton, B. T.: Reduced wind strengthens top-down control of an insect herbivore, Ecology, 95, 2375-2381, doi:10.1890/13-2171.1, 2014.

Bell, V. A., Kay, A. L., Jones, R. G., Moore, R. J., and Reynard, N. S.: Use of soil data in a grid-based hydrological model to estimate spatial variation in changing flood risk across the UK, Journal of Hydrology, 377, 335-350, doi:10.1016/j.jhydrol.2009.08.031, 2009.

Bell, V. A., Gedney, N., Kay, A. L., Smith, R. N. B., Jones, R. G., and Moore, R. J.: Estimating Potential Evaporation from Vegetated Surfaces for Water Management Impact Assessments Using Climate Model Output, Journal of Hydrometeorology, 12, 1127-1136, doi:10.1175/2011jhm1379.1, 2011.

Bell, V. A., Kay, A. L., Cole, S. J., Jones, R. G., Moore, R. J., and Reynard, N. S.: How might climate change affect river flows across the Thames Basin? An area-wide analysis using the UKCP09 Regional Climate Model ensemble, Journal of Hydrology, 442-443, 89-104, doi:10.1016/j.jhydrol.2012.04.001, 2012.

Bellamy, P. H., Loveland, P. J., Bradley, R. I., Lark, R. M., and Kirk, G. J.: Carbon losses from all soils across England and Wales 1978-2003, Nature, 437, 245-248, doi:10.1038/nature04038, 2005.

Berry, P. M., Dawson, T. P., Harrison, P. A., and Pearson, R. G.: Modelling potential impacts of climate change on the bioclimatic envelope of species in Britain and Ireland, Global Ecol Biogeogr, 11, 453-462, doi:10.1046/j.1466-822x.2002.00304.x, 2002.

Best, M. J., Pryor, M., Clark, D. B., Rooney, G. G., Essery, R. L. H., Ménard, C. B., Edwards, J. M., Hendry, M. A., Porson, A., Gedney, N., Mercado, L. M., Sitch, S., Blyth, E., Boucher, O., Cox, P. M., Grimmond, C. S. B., and Harding, R. J.: The Joint UK Land Environment Simulator (JULES), model description – Part 1: Energy and water fluxes, Geoscientific Model Development, 4, 677-699, doi:10.5194/gmd-4-677-2011, 2011.

Brittain, C., Kremen, C., and Klein, A.-M.: Biodiversity buffers pollination from changes in environmental conditions, Global Change Biology, 19, 540-547, doi:10.1111/gcb.12043, 2013.

Burch, S. F., and Ravenscroft, F.: Computer modelling of the UK wind energy resource: Final overview report., AEA Industrial Technology, 1992.

Burt, T. P., and Shahgedanova, M.: An historical record of evaporation losses since 1815 calculated using long-term observations from the Radcliffe Meteorological Station, Oxford, England, Journal of Hydrology, 205, 101-111, doi:10.1016/S0022-1694(97)00143-1, 1998.

Clark, D. B., Mercado, L. M., Sitch, S., Jones, C. D., Gedney, N., Best, M. J., Pryor, M., Rooney, G. G., Essery, R. L. H., Blyth, E., Boucher, O., Harding, R. J., Huntingford, C., and Cox, P. M.: The Joint UK Land Environment Simulator (JULES), model description – Part 2: Carbon fluxes and vegetation dynamics, Geoscientific Model Development, 4, 701-722, doi:10.5194/gmd-4-701-2011, 2011.

Cowley, J. P.: The distribution over Great Britain of global solar irradiation on a horizontal surface, Meteorological Magazine, 107, 357-372, 1978.

Crane, S. B., and Hudson, J. A.: The impact of site factors and climate variability on the calculation of potential evaporation at Moel Cynnedd, Plynlimon, Hydrol. Earth Syst. Sci., 1, 429-445, doi:10.5194/hess-1-429-1997, 1997.

Crooks, S. M., and Naden, P. S.: CLASSIC: a semi-distributed rainfall-runoff modelling system, Hydrol. Earth Syst. Sci., 11, 516-531, doi:10.5194/hess-11-516-2007, 2007.

Crooks, S. M., and Kay, A. L.: Simulation of river flow in the Thames over 120 years: Evidence of change in rainfall-runoff response?, Journal of Hydrology: Regional Studies, 4, Part B, 172-195, doi:10.1016/j.ejrh.2015.05.014, 2015.

Dilley, A. C., and O'Brien, D. M.: Estimating downward clear sky long-wave irradiance at the surface from screen temperature and precipitable water, Quarterly Journal of the Royal Meteorological Society, 124, 1391-1401, doi:10.1256/Smsqj.54902, 1998.

Donohue, R. J., McVicar, T. R., and Roderick, M. L.: Assessing the ability of potential evaporation formulations to capture the dynamics in evaporative demand within a changing climate, Journal of Hydrology, 386, 186-197, doi:10.1016/j.jhydrol.2010.03.020, 2010.

Evans, N., Baierl, A., Semenov, M. A., Gladders, P., and Fitt, B. D.: Range and severity of a plant disease increased by global warming, Journal of the Royal Society, Interface / the Royal Society, 5, 525-531, doi:10.1098/rsif.2007.1136, 2008.

FAO/IIASA/ISRIC/ISS-CAS/JRC: Harmonized World Soil Database, 2012.

Folland, C. K., Hannaford, J., Bloomfield, J. P., Kendon, M., Svensson, C., Marchant, B. P., Prior, J., and Wallace, E.: Multi-annual droughts in the English Lowlands: a review of their characteristics and climate drivers in the winter half-year, Hydrology and Earth System Sciences, 19, 2353-2375, doi:10.5194/hess-19-2353-2015, 2015.

Gedney, N., Cox, P. M., Betts, R. A., Boucher, O., Huntingford, C., and Stott, P. A.: Detection of a direct carbon dioxide effect in continental river runoff records, Nature, 439, 835-838, doi:10.1038/nature04504, 2006.

Gedney, N., Huntingford, C., Weedon, G. P., Bellouin, N., Boucher, O., and Cox, P. M.: Detection of solar dimming and brightening effects on Northern Hemisphere river flow, Nature Geoscience, 7, 796-800, doi:10.1038/ngeo2263, 2014.

Gill, A. E.: Atmosphere-ocean Dynamics, Academic Press, San Diego, California, USA, 1982.

Hannaford, J., and Buys, G.: Trends in seasonal river flow regimes in the UK, Journal of Hydrology, 475, 158-174, doi:10.1016/j.jhydrol.2012.09.044, 2012.

Hannaford, J.: Climate-driven changes in UK river flows: A review of the evidence, Progress in Physical Geography, 39, 29-48, doi:10.1177/0309133314536755, 2015.

Harris, I., Jones, P. D., Osborn, T. J., and Lister, D. H.: Updated high-resolution grids of monthly climatic observations - the CRU TS3.10 Dataset, International Journal of Climatology, 34, 623-642, doi:10.1002/Joc.3711, 2014.

Hartmann, D. L., Klein Tank, A. M. G., Rusticucci, M., Alexander, L. V., Brönnimann, S., Charabi, Y., Dentener, F. J., Dlugokencky, E. J., Easterling, D. R., Kaplan, A., Soden, B. J., Thorne, P. W., Wild, M., and Zhai, P. M.: Observations: Atmosphere and Surface, in: Climate Change 2013: The Physical Science Basis. Contribution of Working Group I to the Fifth Assessment Report of the Intergovernmental Panel on Climate Change, edited by: Stocker, T. F., Qin, D., Plattner, G.-K., Tignor, M., Allen, S. K., Boschung, J., Nauels, A., Xia, Y., Bex, V., and Midgley, P. M., Cambridge University Press, Cambridge, United Kingdom and New York, NY, USA, 159–254, 2013.

Helmes, L., and Jaenicke, R.: Atmospheric turbidity determined from sunshine records, Journal of Aerosol Science, 17, 261-263, doi:10.1016/0021-8502(86)90080-7, 1986.

Hickling, R., Roy, D. B., Hill, J. K., Fox, R., and Thomas, C. D.: The distributions of a wide range of taxonomic groups are expanding polewards, Global Change Biology, 12, 450-455, doi:10.1111/j.1365-2486.2006.01116.x, 2006.

Horn, B. K. P.: Hill Shading and the Reflectance Map, P Ieee, 69, 14-47, doi:10.1109/Proc.1981.11918, 1981.

Hough, M. N., and Jones, R. J. A.: The United Kingdom Meteorological Office rainfall and evaporation calculation system: MORECS version 2.0-an overview, Hydrology and Earth System Sciences, 1, 227-239, doi:10.5194/hess-1-227-1997, 1997.

Iqbal, M.: An introduction to solar radiation, Academic Press, London, 1983.

Jenkins, G. J., Perry, M. C., and Prior, M. J.: The climate of the United Kingdom and recent trends, Met Office Hadley Centre, Exeter, UK, 2008.

Jones, P. D., Lister, D. H., Osborn, T. J., Harpham, C., Salmon, M., and Morice, C. P.: Hemispheric and large-scale land-surface air temperature variations: An extensive revision and an update to 2010, Journal of Geophysical Research: Atmospheres, 117, n/a-n/a, doi:10.1029/2011JD017139, 2012.

Jones, P. D., and Harris, I.: CRU TS3.21: Climatic Research Unit (CRU) Time-Series (TS) Version 3.21 of High Resolution Gridded Data of Month-by-month Variation in Climate (Jan. 1901- Dec. 2012). University of East Anglia Climatic Research Unit, doi:10.5285/D0E1585D-3417-485F-87AE-4FCECF10A992, 2013.

Kay, A. L., Bell, V. A., Blyth, E. M., Crooks, S. M., Davies, H. N., and Reynard, N. S.: A hydrological perspective on evaporation: historical trends and future projections in Britain, Journal of Water and Climate Change, 4, 193, doi:10.2166/wcc.2013.014, 2013.

Kay, A. L., Rudd, A. C., Davies, H. N., Kendon, E. J., and Jones, R. G.: Use of very high resolution climate model data for hydrological modelling: baseline performance and future flood changes, Climatic Change, doi:10.1007/s10584-015-1455-6, 2015.

Keller, V. D. J., Tanguy, M., Prosdocimi, I., Terry, J. A., Hitt, O., Cole, S. J., Fry, M., Morris, D. G., and Dixon, H.: CEH-GEAR: 1 km resolution daily and monthly areal rainfall estimates for the UK for hydrological and other applications, Earth Syst. Sci. Data, 7, 143-155, doi:10.5194/essd-7-143-2015, 2015.

Hydrol. Earth Syst. Sci. Discuss., doi:10.5194/hess-2015-520, 2016
Manuscript under review for journal Hydrol. Earth Syst. Sci.
Published: 27 January 2016




Kimball, B. A., Idso, S. B., and Aase, J. K.: A Model of Thermal-Radiation from Partly Cloudy and Overcast Skies, Water Resources Research, 18, 931-936, doi:10.1029/Wr018i004p00931, 1982.

Kruijt, B., Witte, J.-P. M., Jacobs, C. M. J., and Kroon, T.: Effects of rising atmospheric CO2 on evapotranspiration and soil moisture: A practical approach for the Netherlands, Journal of Hydrology, 349, 257-267, doi:10.1016/j.jhydrol.2007.10.052, 2008.

Liley, J. B.: New Zealand dimming and brightening, Journal of Geophysical Research, 114, doi:10.1029/2008jd011401, 2009.

Marsh, T., and Dixon, H.: The UK water balance – how much has it changed in a warming world?, 01-05, doi:10.7558/bhs.2012.ns32, 2012.

Matsoukas, C., Benas, N., Hatzianastassiou, N., Pavlakis, K. G., Kanakidou, M., and Vardavas, I.: Potential evaporation trends over land between 1983–2008: driven by radiative fluxes or vapour-pressure deficit?, Atmospheric Chemistry and Physics, 11, 7601-7616, doi:10.5194/acp-11-7601-2011, 2011.

McVicar, T. R., Roderick, M. L., Donohue, R. J., Li, L. T., Van Niel, T. G., Thomas, A., Grieser, J., Jhajharia, D., Himri, Y., Mahowald, N. M., Mescherskaya, A. V., Kruger, A. C., Rehman, S., and Dinpashoh, Y.: Global review and synthesis of trends in observed terrestrial near-surface wind speeds: Implications for evaporation, Journal of Hydrology, 416, 182-205, doi:10.1016/j.jhydrol.2011.10.024, 2012.

Monteith, J. L.: Evaporation and environment, in: 19th Symposia of the Society for Experimental Biology, University Press, Cambridge, 1965.

Morris, D. G., and Flavin, R. W.: A digital terrain model for hydrology., Proceedings of the 4th International Symposium on Spatial Data Handling, 1, 250-262, 1990.

Morton, D., Rowland, C., Wood, C., Meek, L., Marston, C., Smith, G., Wadsworth, R., and Simpson, I. C.: Final Report for LCM2007 - the new UK land cover map, NERC/Centre for Ecology & Hydrology 11/07 (CEH Project Number: C03259), 2011.

Muneer, T., and Munawwar, S.: Potential for improvement in estimation of solar diffuse irradiance, Energ Convers Manage, 47, 68-86, doi:10.1016/j.enconman.2005.03.015, 2006.

Murphy, J. M., Sexton, D. M. H., Jenkins, G. J., Boorman, P. M., Booth, B. B. B., Brown, C. C., Clark, R. T., Collins, M., Harris, G. R., Kendon, E. J., Betts, R. A., Brown, S. J., Howard, T. P., Humphrey, K. A., McCarthy, M. P., McDonald, R. E., Stephens, A., Wallace, C., Warren, R., Wilby, R., and Wood, R. A.: UK Climate Projections Science Report: Climate change projections, Met Office Hadley Centre, Exeter, 2009.

Newton, K., and Burch, S. F.: Estimation of the UK wind energy resource using computer modelling techniques and map data, Energy Technology Support Unit, 50, 1985.

Norton, L. R., Maskell, L. C., Smart, S. S., Dunbar, M. J., Emmett, B. A., Carey, P. D., Williams, P., Crowe, A., Chandler, K., Scott, W. A., and Wood, C. M.: Measuring stock and change in the GB countryside for policy--key findings and developments from the Countryside Survey 2007 field survey, Journal of environmental management, 113, 117-127, doi:10.1016/j.jenvman.2012.07.030, 2012.

Palmer, W. C.: Meteorological Drought. Res. Paper No.45, Dept. of Commerce, Washington, D.C., 1965.

Parker, D., and Horton, B.: Uncertainties in central England temperature 1878-2003 and some improvements to the maximum and minimum series, International Journal of Climatology, 25, 1173-1188, doi:10.1002/joc.1190, 2005.

Pocock, M. J., Roy, H. E., Preston, C. D., and Roy, D. B.: The Biological Records Centre in the United Kingdom: a pioneer of citizen science., Biological Journal of the Linnean Society, doi:10.1111/bij.12548, 2015.

Prata, A. J.: A new long-wave formula for estimating downward clear-sky radiation at the surface, Quarterly Journal of the Royal Meteorological Society, 122, 1127-1151, doi:10.1002/qj.49712253306, 1996.

Prescott, J. A.: Evaporation from a water surface in relation to solar radiation, Transaction of the Royal Society of South Australia, 64, 114-125, 1940.

Prudhomme, C., Giuntoli, I., Robinson, E. L., Clark, D. B., Arnell, N. W., Dankers, R., Fekete, B. M., Franssen, W., Gerten, D., Gosling, S. N., Hagemann, S., Hannah, D. M., Kim, H., Masaki, Y., Satoh, Y., Stacke, T., Wada, Y., and Wisser, D.: Hydrological droughts in the 21st century, hotspots and uncertainties from a global multimodel ensemble experiment, Proceedings of the National Academy of Sciences, 111, 3262-3267, doi:10.1073/pnas.1222473110, 2014.

Reynolds, B., Chamberlain, P. M., Poskitt, J., Woods, C., Scott, W. A., Rowe, E. C., Robinson, D. A., Frogbrook, Z. L., Keith, A. M., Henrys, P. A., Black, H. I. J., and Emmett, B. A.: Countryside Survey: National "Soil Change" 1978–2007 for Topsoils in Great Britain—Acidity, Carbon, and Total Nitrogen Status, Vadose Zone Journal, 12, 0, doi:10.2136/vzj2012.0114, 2013.

Richards, J. M.: A simple expression for the saturation vapour pressure of water in the range −50 to 140°C, Journal of Physics D: Applied Physics, 4, L15, 1971.

Robinson, E. L., Blyth, E., Clark, D. B., Finch, J., and Rudd, A. C.: Climate hydrology and ecology research support system potential evapotranspiration dataset for Great Britain (1961-2012) [CHESS-PE], NERC-Environmental Information Data Centre, 2015a.

Robinson, E. L., Blyth, E., Clark, D. B., Finch, J., and Rudd, A. C.: Climate hydrology and ecology research support system meteorology dataset for Great Britain (1961-2012) [CHESS-met], NERC-Environmental Information Data Centre, 2015b.

Rodda, J. C., and Marsh, T. J.: The 1975-76 Drought - a contemporary and retrospective review, Wallingford, UK, 2011.

Rudd, A. C., and Kay, A. L.: Use of very high resolution climate model data for hydrological modelling: estimation of potential evaporation, Hydrology Research, doi: 10.2166/nh.2015.028, 2015.

Rutter, A. J., Kershaw, K. A., Robins, P. C., and Morton, A. J.: A predictive model of rainfall interception in forests, 1. Derivation of the model from observations in a plantation of Corsican pine, Agricultural Meteorology, 9, 367-384, doi:10.1016/0002-1571(71)90034-3, 1971.

Sanchez-Lorenzo, A., Calbó, J., and Martin-Vide, J.: Spatial and Temporal Trends in Sunshine Duration over Western Europe (1938–2004), Journal of Climate, 21, 6089-6098, doi:10.1175/2008jcli2442.1, 2008.

Sanchez-Lorenzo, A., Calbó, J., Brunetti, M., and Deser, C.: Dimming/brightening over the Iberian Peninsula: Trends in sunshine duration and cloud cover and their relations with atmospheric circulation, Journal of Geophysical Research, 114, doi:10.1029/2008jd011394, 2009.

Sanchez-Lorenzo, A., and Wild, M.: Decadal variations in estimated surface solar radiation over Switzerland since the late 19th century, Atmospheric Chemistry and Physics, 12, 8635-8644, doi:10.5194/acp-12-8635-2012, 2012.

Sanchez-Romero, A., Sanchez-Lorenzo, A., Calbó, J., González, J. A., and Azorin-Molina, C.: The signal of aerosol-induced changes in sunshine duration records: A review of the evidence, Journal of Geophysical Research: Atmospheres, 119, 4657-4673, doi:10.1002/2013JD021393, 2014.

Sheffield, J., Goteti, G., and Wood, E. F.: Development of a 50-Year High-Resolution Global Dataset of Meteorological Forcings for Land Surface Modeling, Journal of Climate, 19, 3088-3111, doi:10.1175/JCLI3790.1, 2006.

Shuttleworth, W. J.: Terrestrial Hydrometeorology, John Wiley & Sons, Ltd, 2012.

Sinden, G.: Characteristics of the UK wind resource: Long-term patterns and relationship to electricity demand, Energy Policy, 35, 112-127, doi:10.1016/j.enpol.2005.10.003, 2007.

Stanhill, G., and Cohen, S.: Solar Radiation Changes in the United States during the Twentieth Century: Evidence from Sunshine Duration Measurements, Journal of Climate, 18, 1503-1512, doi:10.1175/JCLI3354.1, 2005.

Stanhill, G., and Möller, M.: Evaporative climate change in the British Isles, International Journal of Climatology, 28, 1127-1137, doi:10.1002/joc.1619, 2008.

Stewart, J. B.: On the use of the Penman-Monteith equation for determining areal evapotranspiration, in: Estimation of Areal Evapotranspiration (Proceedings of a workshop held at Vancouver, B.C., Canada, August 1987). edited by: Black, T. A. S., D. L.; Novak, M. D.; Price, D. T., IAHS, Wallingford, Oxfordshire, UK, 1989.

Sutton, R. T., and Dong, B.: Atlantic Ocean influence on a shift in European climate in the 1990s, Nature Geosci, 5, 788-792, doi:10.1038/ngeo1595, 2012.

Tanguy, M., Dixon, H., Prosdocimi, I., Morris, D. G., and Keller, V. D. J.: Gridded estimates of daily and monthly areal rainfall for the United Kingdom (1890-2012) [CEH-GEAR], NERC Environmental Information Data Centre, doi:10.5285/5dc179dc-f692-49ba-9326-a6893a503f6e, 2014.

Thackeray, S. J., Sparks, T. H., Frederiksen, M., Burthe, S., Bacon, P. J., Bell, J. R., Botham, M. S., Brereton, T. M., Bright, P. W., Carvalho, L., Clutton-Brock, T., Dawson, A., Edwards, M., Elliott, J. M., Harrington, R., Johns, D., Jones, I. D., Jones, J. T., Leech, D. I., Roy, D. B., Scott, W. A., Smith, M., Smithers, R. J., Winfield, I. J., and Wanless, S.: Trophic level asynchrony in rates of phenological change for marine, freshwater and terrestrial environments, Global Change Biology, 16, 3304-3313, doi:10.1111/j.1365-2486.2010.02165.x, 2010.

Thompson, N., Barrie, I. A., and Ayles, M.: The Meteorological Office rainfall and evaporation calculation system: MORECS, Meteorological Office, Bracknell, 1981.

Vautard, R., Cattiaux, J., Yiou, P., Thepaut, J. N., and Ciais, P.: Northern Hemisphere atmospheric stilling partly attributed to an increase in surface roughness, Nature Geoscience, 3, 756-761, doi:10.1038/Ngeo979, 2010.

Hydrol. Earth Syst. Sci. Discuss., doi:10.5194/hess-2015-520, 2016
Manuscript under review for journal Hydrol. Earth Syst. Sci.
Published: 27 January 2016


von Storch, H., and Zwiers, F. W.: Statistical analysis in climate research, Cambridge University Press, Cambridge ; New York, x, 484 p. pp., 1999.

Wang, K., and Liang, S.: Global atmospheric downward longwave radiation over land surface under all-sky conditions from 1973 to 2008, Journal of Geophysical Research, 114, doi:10.1029/2009jd011800, 2009.

Ward, R. C., and Robinson, M.: Principles of Hydrology, McGraw Hill, 2000.

Watts, G., Battarbee, R. W., Bloomfield, J. P., Crossman, J., Daccache, A., Durance, I., Elliott, J. A., Garner, G., Hannaford, J., Hannah, D. M., Hess, T., Jackson, C. R., Kay, A. L., Kernan, M., Knox, J., Mackay, J., Monteith, D. T., Ormerod, S. J., Rance, J., Stuart, M. E., Wade, A. J., Wade, S. D., Weatherhead, K., Whitehead, P. G., and Wilby, R. L.: Climate change and water in the UK - past changes and future prospects, Progress in Physical Geography, 39, 6-28, doi:10.1177/0309133314542957, 2015.

Weedon, G. P., Gomes, S., Viterbo, P., Shuttleworth, W. J., Blyth, E., Osterle, H., Adam, J. C., Bellouin, N., Boucher, O., and Best, M.: Creation of the WATCH Forcing Data and Its Use to Assess Global and Regional Reference Crop Evaporation over Land during the Twentieth Century, Journal of Hydrometeorology, 12, 823-848, doi:10.1175/2011jhm1369.1, 2011.

Weedon, G. P., Balsamo, G., Bellouin, N., Gomes, S., Best, M. J., and Viterbo, P.: The WFDEI meteorological forcing data set: WATCH Forcing Data methodology applied to ERA-Interim reanalysis data, Water Resources Research, 50, 7505-7514, doi:10.1002/2014WR015638, 2014.

Wild, M.: Global dimming and brightening: A review, Journal of Geophysical Research, 114, doi:10.1029/2008jd011470, 2009.

Wood, C. M., Smart, S. M., and Bunce, R. G. H.: Woodland survey of Great Britain 1971–2001, Earth System Science Data Discussions, 8, 259-277, doi:10.5194/essdd-8-259-2015, 2015.

Zwiers, F. W., and von Storch, H.: Taking Serial-Correlation into Account in Tests of the Mean, Journal of Climate, 8, 336-351, doi:10.1175/1520-0442(1995)008<0336:Tsciai>2.0.Co;2, 1995.

Hydrol. Earth Syst. Sci. Discuss., doi:10.5194/hess-2015-520, 2016
Manuscript under review for journal Hydrol. Earth Syst. Sci.
Published: 27 January 2016


Hydrology and Earth System Sciences
Open Access
Discussions

1 Table 1. Variable details

| Variable (units) | Source data | Ancillary files | Assumptions | Height |
|---|---|---|---|---|
| Air temperature (K) | MORECS air temperature | IHDTM elevation | Lapsed to IHDTM elevation | 1.2 m |
| Specific humidity (kg kg$^{-1}$) | MORECS vapour pressure, air temperature | IHDTM elevation | Lapsed to IHDTM elevation<br>Constant air pressure | 1.2 m |
| Downward longwave radiation (W m$^{-2}$) | MORECS air temperature, vapour pressure, sunshine hours | IHDTM elevation | Constant cloud base height | n/a |
| Downward shortwave radiation (W m$^{-2}$) | MORECS sunshine hours | IHDTM elevation<br>Spatially-varying aerosol correction | No time-varying aerosol correction | n/a |
| Wind speed (m s$^{-1}$) | MORECS wind speed | ETSU average wind speeds | Wind speed correction is constant | 10 m |
| Precipitation (kg m$^{-2}$ s$^{-1}$) | CEH-GEAR precipitation | | No transformations performed | n/a |
| Daily temperature range (K) | CRU TS 3.21 daily temperature range | | No spatial interpolation from 0.5° resolution.<br>No temporal interpolation (constant values for each month) | 1.2 m |

Hydrol. Earth Syst. Sci. Discuss., doi:10.5194/hess-2015-520, 2016
Manuscript under review for journal Hydrol. Earth Syst. Sci.
Published: 27 January 2016

Hydrology and Earth System Sciences
Open Access
Discussions

| | | | | |
|---|---|---|---|---|
| Surface air pressure (Pa) | WFD air pressure | IHDTM elevation | Mean-monthly values from WFD used (each year has same values). Lapsed to IHDTM elevation. No temporal interpolation (constant values for each month). | n/a |

Hydrol. Earth Syst. Sci. Discuss., doi:10.5194/hess-2015-520, 2016
Manuscript under review for journal Hydrol. Earth Syst. Sci.
Published: 27 January 2016

Hydrology and Earth System Sciences
Open Access
Discussions

Table 2: Rate of change of annual means of meteorological and potential evapotranspiration variables in Great Britain. Bold indicates trends that are significant at the 5% level. Numbers in brackets show the 95% confidence intervals.

| Variable | Rate of change (95% confidence interval) |
|---|---|
| Air temperature | **0.20 (0.07, 0.31) K decade$^{-1}$** |
| Specific humidity | **0.046 (0.010, 0.082) g kg$^{-1}$ decade$^{-1}$** |
| Downward shortwave radiation | **1.1 (0.3, 1.8) W m$^{-2}$ decade$^{-1}$** |
| Downward longwave radiation | 0.45 (-0.01,0.91) W m$^{-2}$ decade$^{-1}$ |
| Wind speed | -0.17 (-0.27, -0.08) m s$^{-1}$ decade$^{-1}$ |
| Precipitation | **0.08 (0.02, 0.14) mm day$^{-1}$ decade$^{-1}$** |
| Daily temperature range | -0.06 (-0.12,0.00) K decade$^{-1}$ |
| PET | **0.021 (0.00,0.041) mm day$^{-1}$ decade$^{-1}$** |
| PETI | 0.019 (0.00,0.039) mm day$^{-1}$ decade$^{-1}$ |

Hydrol. Earth Syst. Sci. Discuss., doi:10.5194/hess-2015-520, 2016
Manuscript under review for journal Hydrol. Earth Syst. Sci.
Published: 27 January 2016

Hydrology and Earth System Sciences
Open Access
Discussions

Table 3. Percentage contribution of the trend in each variable to the trends in annual mean PET and its radiative and aerodynamic components.

| a) Potential evapotranspiration (PET) | | | | | |
|---|---|---|---|---|---|
| | Air temperature | Specific humidity | Wind speed | Downward longwave | Downward shortwave |
| England | 7.7 % | -4.6 % | -1.8 % | 26.4 % | 72.3 % |
| Scotland | 9.2 % | -6.0 % | -3.2 % | 53.4 % | 46.5 % |
| Wales | 8.2 % | -5.6 % | -2.4 % | 32.7 % | 67.0 % |
| English lowlands | 7.3 % | -4.0 % | -1.4 % | 22.7 % | 75.3 % |
| Great Britain | 8.1 % | -5.1 % | -2.2 % | 33.9 % | 65.3 % |
| **b) Radiative component of PET** | | | | | |
| | Air temperature | Specific humidity | Wind speed | Downward longwave | Downward shortwave |
| England | -1.6 % | n/a | 1.5 % | 26.8 % | 73.3 % |
| Scotland | -1.9 % | n/a | 2.5 % | 53.1 % | 46.3 % |
| Wales | -1.5 % | n/a | 2.8 % | 32.3 % | 66.3 % |
| English lowlands | -1.7 % | n/a | 1.1 % | 23.3 % | 77.2 % |
| Great Britain | -1.7 % | n/a | 1.9 % | 34.1 % | 65.7 % |
| **c) Aerodynamic component of PET** | | | | | |
| | Air temperature | Specific humidity | Wind speed | Downward longwave | Downward shortwave |
| England | 703.7 % | -353.5 % | -250.2 % | n/a | n/a |
| Scotland | -1210.0 % | 662.2 % | 647.3 % | n/a | n/a |
| Wales | -854.7 % | 492.3 % | 462.5 % | n/a | n/a |
| English lowlands | 365.4 % | -165.8 % | -99.6 % | n/a | n/a |
| Great Britain | 2025.0 % | -1061.9 % | -863.1 % | n/a | n/a |

Hydrology and Earth System Sciences
Open Access
Discussions

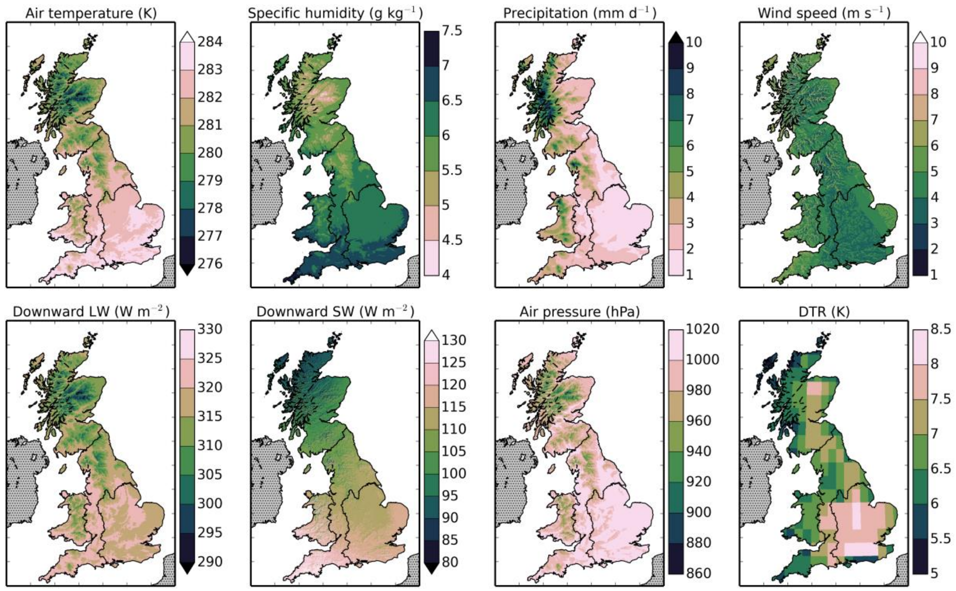


Figure 1. Means of the meteorological variables over the years 1961-2012. Top row, left to right are 1.2 m air temperature, 1.2 m specific humidity, precipitation, 10 m wind speed. Bottom row left to right are downward longwave radiation, downward shortwave radiation, surface air pressure, daily air temperature range.

Hydrol. Earth Syst. Sci. Discuss., doi:10.5194/hess-2015-520, 2016
Manuscript under review for journal Hydrol. Earth Syst. Sci.
Published: 27 January 2016


Hydrology and Earth System Sciences
Open Access
Discussions

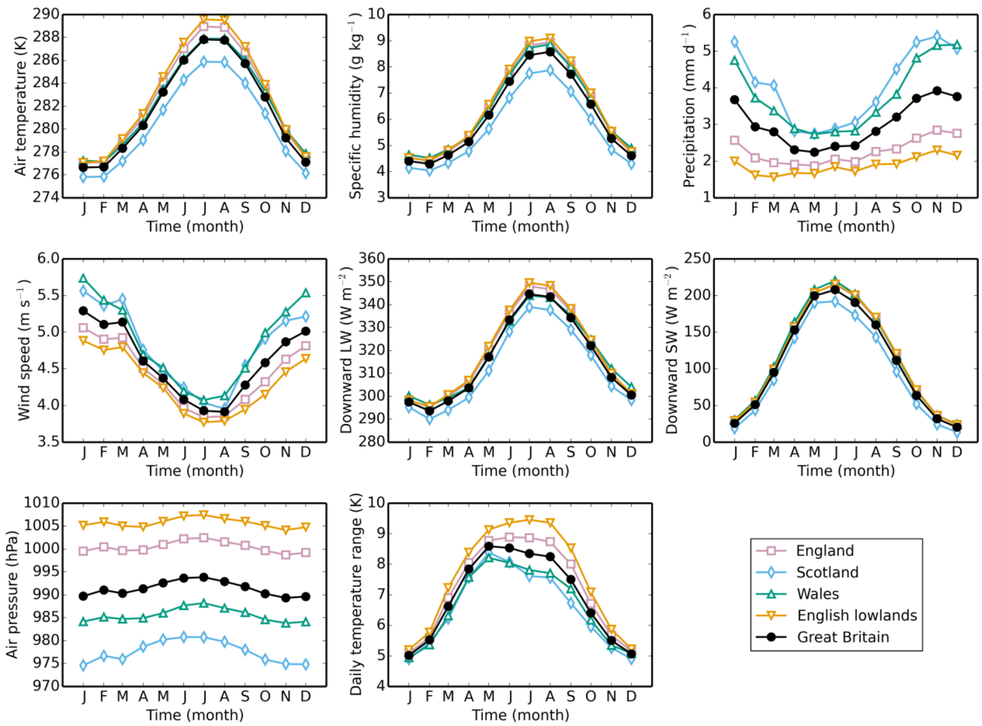


Figure 2. Mean monthly climatology of meteorological variables for five different regions of Great Britain, calculated over the years 1961-2012.

Hydrol. Earth Syst. Sci. Discuss., doi:10.5194/hess-2015-520, 2016
Manuscript under review for journal Hydrol. Earth Syst. Sci.
Published: 27 January 2016


Hydrology and Earth System Sciences
Open Access
Discussions

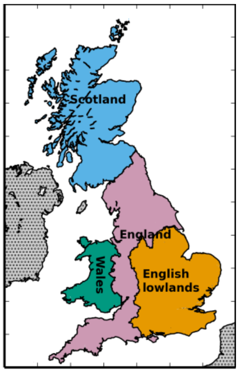


Figure 3. The regions used to calculate the area means. The English lowlands are a sub-region of England. England, Scotland and Wales together form the fifth region, Great Britain.

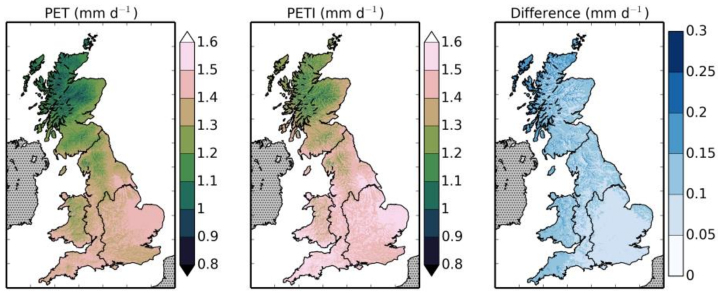


Figure 4. Mean PET (right), mean PETI (centre), and the difference between mean PETI and PET (right), calculated over the years 1961-2012.

Hydrol. Earth Syst. Sci. Discuss., doi:10.5194/hess-2015-520, 2016
Manuscript under review for journal Hydrol. Earth Syst. Sci.
Published: 27 January 2016


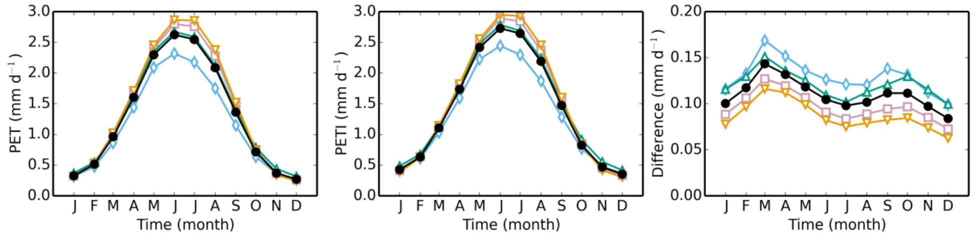


Figure 5. Mean monthly climatology of PET (left), PETI (centre) and the difference PETI-PET (right) for five different regions of Great Britain, calculated over the years 1961-2012. Symbols as in Fig. 2.

Hydrol. Earth Syst. Sci. Discuss., doi:10.5194/hess-2015-520, 2016
Manuscript under review for journal Hydrol. Earth Syst. Sci.
Published: 27 January 2016



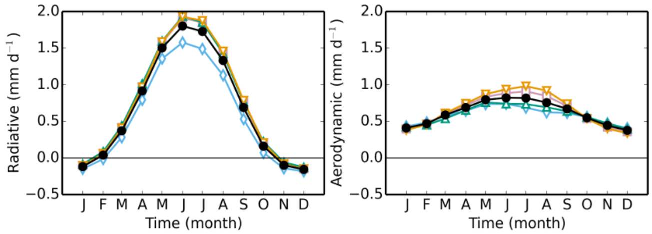


Figure 6. Mean-monthly climatology of the radiative (left) and aerodynamic (right) components of the PET for five different regions of Great Britain, calculated over the years 1961-2012. Symbols as in Fig. 2.

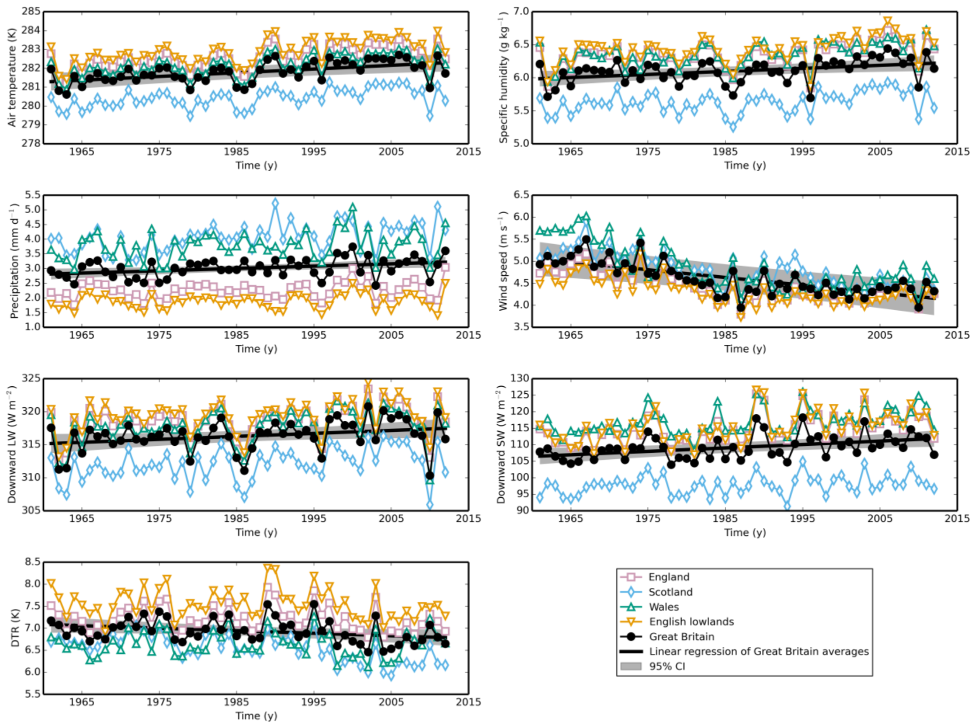


Figure 7. Annual means of the meteorological variables over five regions of Great Britain. The solid black lines show the linear regression fit to the Great Britain annual means, while the grey strip shows the 95% confidence interval of the same fit, assuming a non-zero lag-1 correlation coefficient.

Hydrol. Earth Syst. Sci. Discuss., doi:10.5194/hess-2015-520, 2016
Manuscript under review for journal Hydrol. Earth Syst. Sci.
Published: 27 January 2016


Hydrology and Earth System Sciences
Discussions

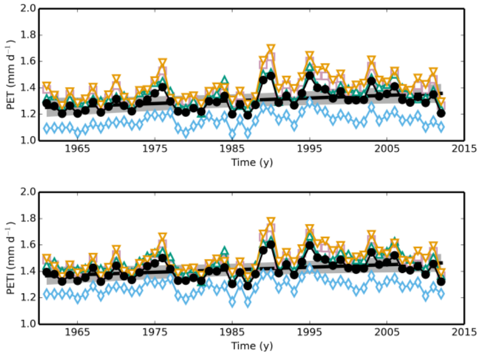


Figure 8. Annual means of PET and PETI for five regions of Great Britain. Symbols as in Fig. 7.

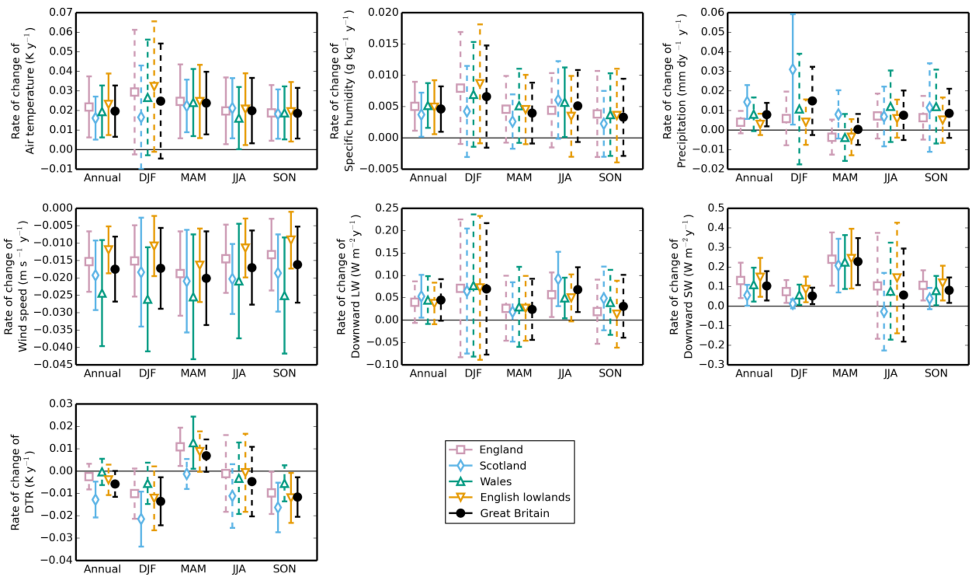


Figure 9. Rate of change of annual and seasonal means of meteorological variables for five regions of Great Britain for the years 1961-2012. Error bars are the 95% confidence intervals calculated assuming a non-zero lag-1 correlation coefficient. Solid error bars indicate slopes that are statistically significant at the 5% level, dashed error bars indicate slopes that are not significant at the 5% level.

Hydrol. Earth Syst. Sci. Discuss., doi:10.5194/hess-2015-520, 2016
Manuscript under review for journal Hydrol. Earth Syst. Sci.
Published: 27 January 2016


Hydrology and Earth System Sciences
Open Access
Discussions

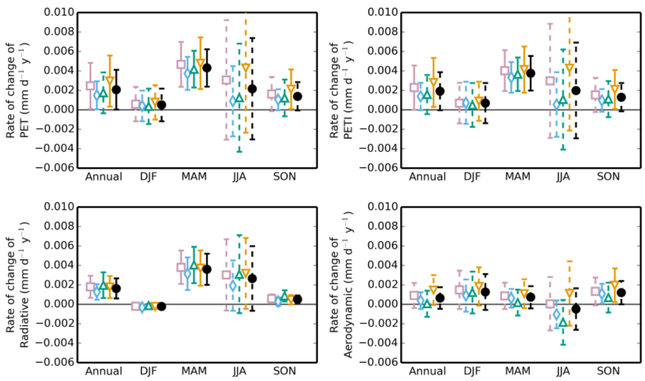


Figure 10. Rate of change of annual and seasonal means of PET (top left), PETI (top right), the radiative component of PET (lower left) and the aerodynamic component of PET (lower right) for five regions of Great Britain for the years 1961-2012. Symbols as in Fig. 9.

Hydrology and Earth System Sciences
Open Access
Discussions

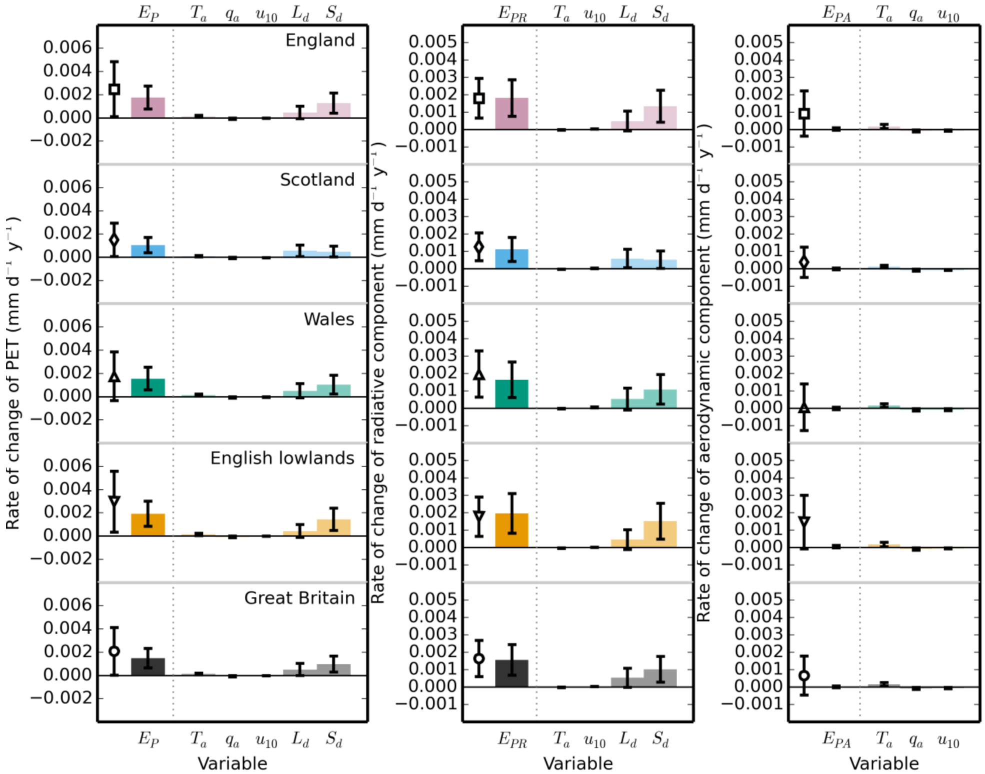


Figure 11. The contribution of the rate of change of each meteorological variable to the rate of change of PET (left), the radiative component (centre) and the aerodynamic component (right). In each panel the left hand bar is the rate of change of PET derived from the rate of change of each of the variables. The rest of the columns show the contribution to that change from each of the variables. The error bars show the 95% confidence intervals on each value. For the left hand bar, the symbols with error bars show the slope and its associated confidence interval obtained from the linear regression (as in Fig. 10).